

# ON THE MINIMUM DILATATION PROBLEM FOR PSEUDO-ANOSOV BRAIDS

ANDREW ZENG

ABSTRACT. In this article, we study pseudo-Anosov braids. We develop methods for showing a lower bound of their dilatations inspired by the works of Hironaka-Kin and McMullen. This is the write-up for a research project conducted during summer 2024 at the Université du Québec à Montréal, supervised by Chi Cheuk Tsang.

## 1. ACKNOWLEDGEMENTS

I am grateful to Chi Cheuk Tsang for spending many hours teaching me all about pseudo-Anosov maps during our meetings; He is a great mentor and advisor to have. We had many enlightening discussions throughout the summer, both in-person and over email. Furthermore, through this experience he gave me an introduction to research in mathematics. I am very glad I had the privilege to work on this project.

## 2. INTRODUCTION TO PSEUDO-ANOSOV MAPS

**2.1. Measured singular foliations.** We fix a compact orientable surface  $S$ .

**Definition 2.1.** A **foliation** on  $S$  is a partition  $\mathcal{F}$  of  $S$  into connected one-manifolds such that at each point  $x \in S$ , we may find a chart  $(U, \phi)$  containing  $x$  such that  $\phi(\mathcal{F} \cap U) \cong \sqcup_{y \in \mathbb{R}} \mathbb{R} \times \{y\}$ .

**Definition 2.2.** Each one-manifold above is called a **leaf**.

**Definition 2.3.** A **measured foliation** is a foliation with a measure

$$\mu : \{\text{compact 1-manifolds on } S \text{ nowhere parallel to } \mathbb{F}\} \rightarrow \mathbb{R}_{\geq 0}$$

satisfying the following:

- If  $\alpha_1 + \alpha_2$  is the concatenation of two such one-manifolds, then  $\mu(\alpha_1 + \alpha_2) = \mu(\alpha_1) + \mu(\alpha_2)$
- Let  $F : [0, 1] \times S \rightarrow S$  be an isotopy such that  $F(0, x) = x \ \forall x \in S$  and  $F(t, x) : S \rightarrow S$  is a homeomorphism for each fixed  $t$ . If  $\alpha_1$  (with endpoints  $x_0, x_1$ ) and  $\alpha_2$  are two compact one-manifolds transverse to  $\mathcal{F}$  such that  $F(1, \alpha_1) = \alpha_2$ ,  $\{F(t, x_0) : t \in [0, 1]\}$  belongs to a single leaf in  $\mathcal{F}$ , and  $\{F(t, x_1) : t \in [0, 1]\}$  belongs to a single leaf in  $\mathcal{F}$ , then  $\mu(\alpha_1) = \mu(\alpha_2)$ .

**Definition 2.4.** A **measured singular foliation** is a measured foliation on  $S$  where the foliations locally look like  $\sqcup_{y \in \mathbb{R}} \mathbb{R} \times \{y\}$  except at the **singular points**  $\{p_i\}_{i \in I}$ . At the singular points, the foliation instead locally resembles the pullback of  $\sqcup_{y \in \mathbb{R}} \mathbb{R} \times \{y\}$  by the map  $z \mapsto z^{\frac{n}{2}}$  for some  $n \geq 3$ . We call  $n$  the number of prongs of the singular points.

We will want to introduce a more general notion of a pseudo-Anosov map, on *punctured* surfaces. On a surface  $S$ , let  $\{q_j\}$  be a finite set containing the locations of punctures on the surface.

**Definition 2.5.** A **measured singular foliation on a punctured surface** on  $S$  is a measured foliation on  $S$  where around the singular points  $\{p_i\}_{i \in I}$  the foliation locally looks like the pullback of  $\sqcup_{y \in \mathbb{R}} \mathbb{R} \times \{y\}$  by the map  $z \mapsto z^{\frac{n}{2}}$  for some  $n \geq 3$  as before. However, around the punctures  $\{q_j\}$ , the foliation resembles the pullback of  $\sqcup_{y \in \mathbb{R}} \mathbb{R} \times \{y\}$  by the map  $z \mapsto z^{\frac{n}{2}}$  for some  $n \geq 1$ .

The foliations around a puncture for the case  $n = 1$  will play an outsized role in the later sections.

## 2.2. Pseudo-Anosov maps.

**Definition 2.6.** A *pseudo-Anosov map*  $f : S \rightarrow S$  is a homeomorphism along with a pair of transverse (there are no points of tangency between the leaves of the two foliations) measured singular foliations  $(l^s, \mu^s), (l^u, \mu^u)$ , known as the stable and unstable foliations such that  $f$  takes the leaves of each foliation to the leaves of the same foliation, and stretches or contracts by a factor  $\lambda > 1$  in the transverse direction:

$$\begin{aligned} f(l^s, \mu^s) &= (l^s, \frac{1}{\lambda} \mu^s) \\ f(l^u, \mu^u) &= (l^u, \lambda \mu^u) \end{aligned}$$

**Definition 2.7.**  $\lambda$  is the *dilatation* of  $f$ .

The goal of this article is to make progress towards answering specific cases of the question, *what is the minimum possible dilatation of a pseudo-Anosov map on a given surface?*

It makes sense to ask this question because of the following result:

**Theorem 2.8** ([Iva88, Ivanov]). *On a fixed surface, there are only finitely many pseudo-Anosov maps with dilatation below a certain value, up to conjugation and homotopy.*

## 2.3. Periodic and fixed points.

**Lemma 2.9** ([Tsa24, Page 2]). *The following hold for a pseudo-Anosov map, along with its data of the pair of measured singular foliations:*

- *There is at most one periodic point on a leaf.*
- *The set of periodic points is dense.*

## 3. TRAIN TRACKS

Train tracks are objects that may be used to study the dilatation of pseudo-Anosov maps using tools from graph theory.

Fix a surface  $S$ .

**Definition 3.1.** A *train track* on  $S$  is an embedded undirected graph such that at every point of intersection of the graph, the tangents of the intersecting curves are equal. The edges are often referred to as branches.

**Definition 3.2.** The points of intersection on a train track are its *switches*.

**Definition 3.3.** A *smooth edge path* in a train track is a concatenation of (possibly repeating) branches that does not form cusps.

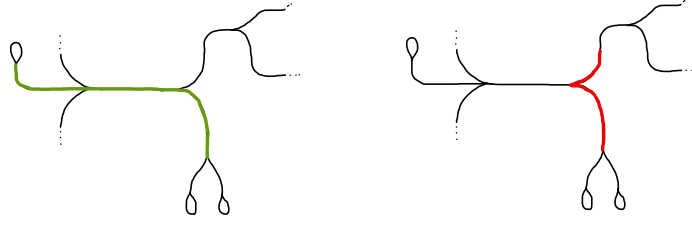


FIGURE 1. The path on the left is a smooth edge path, while the one on the right is not, for two reasons. First, it is not smooth as it contains a cusp. Second, it is not a concatenation of branches, as the the path does not contain the upper branch in its entirety.

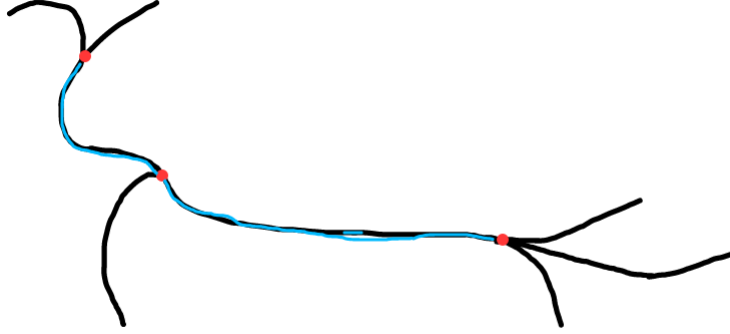


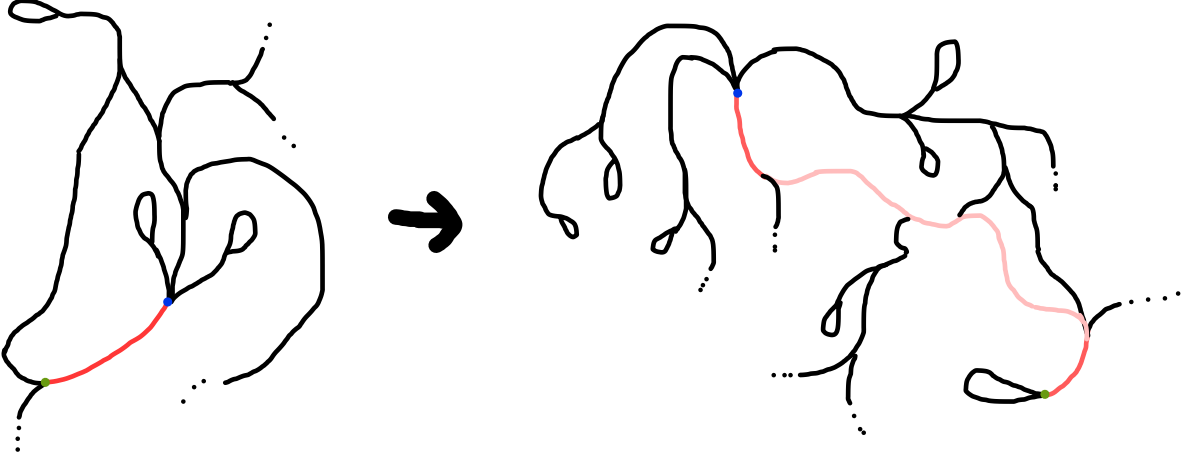
FIGURE 2. The image above shows a subset of a train track. The switches are colored in red and a smooth edge path of two edges/branches is colored in blue. Note that the smooth edge path contains the switch in the middle.

**3.1. Train track maps.** Let  $T$  be a train track on a surface  $S$ .

**Definition 3.4.** A **train track map** of  $T$  is a homeomorphism  $f : S \rightarrow S$  that sends switches to switches and edges to smooth edge paths.

Let there be a train track map  $f : S \rightarrow S$ .

**Definition 3.5.** The **derivative**  $D_f : E(T) \rightarrow E(T)$  of  $f$  is defined as follows: Given a branch  $b \in E(T)$ ,  $f(b)$  is an smooth edge path  $b_1 b_2 \dots b_n$  in  $T$ . The derivative of  $f$  at  $b$  is either  $b_1$  or  $b_n$ , depending on which end of  $b$  is denoted the front of the branch. For example, consider the image below.



Here,  $b$  is the red branch in the image on the left. Under the train track map, it is mapped to the edge path on the right that is colored. If we take the derivative of the map and apply it to  $b$  with the blue point as the front of  $b$ , then the derivative will turn out to be the red branch on the right that is incident to the blue point, and similarly for the green point. Usually we will be implicit in the choice of the front of a branch.

Train track maps satisfy the following condition: if  $e_1$  and  $e_2$  are edges in our train track  $T$  that are both incident to the switch  $s$ , then  $D_f(e_1)$  and  $D_f(e_2)$  are both incident to the switch  $f(s)$ .

Let  $f : S \rightarrow S$  be a train track map of  $T \subset S$

**Definition 3.6.** The **transition matrix** of  $f$  is an  $|E(T)| \times |E(T)|$  non-negative integer matrix that captures information about where  $f$  sends the edges of  $T$ . Label the edges of  $T$   $1, 2, \dots, n = |E(T)|$  and identify each edge with its label as an abuse of notation. Let  $e_1, e_2 \in \{1, 2, \dots, n\}$ . Then the entry at position  $(e_1, e_2)$  of the transition matrix is the number of times  $f(e_2)$  passes through  $e_1$ .

**Definition 3.7.** A square matrix  $A \in M_{n \times n}(\mathbb{R})$  is **Perron-Frobenius** if there exists a  $k \in \mathbb{N}$ : every entry of  $A^k$  is strictly greater than 0.

The main motivation for using train tracks is that given a pseudo-Anosov map on a surface  $S$ , there always exists a train track  $T$  embedded on  $S$  and a train track map  $f : S \rightarrow S$  that is homotopic to the pseudo-Anosov map, and by studying the train track map, we may extract insights about the pseudo-Anosov map.

**3.2. Tie neighbourhoods and Markov partitions.** Let  $T$  be a train track on a surface  $S$ .

**Definition 3.8.** A **tie** of  $T$  is a compact interval on  $S$  containing exactly one point of  $T$ , and is orthogonal to  $T$  at that point.

**Definition 3.9.** A **tie neighbourhood** of  $T$  is a subset of  $S$  that is the union of ties such that each point of  $T$  is covered by a tie.

**Definition 3.10.** A tie containing a switch of the train track is a **switch tie**.

For visual clarity, we usually draw tie neighbourhoods to have a consistent width along each branch, and for the sum of the widths to be equal on each side of a switch tie.

**Definition 3.11.** A train track  $T \subset S$  **carries** a pseudo-Anosov homeomorphism  $f : S \rightarrow S$  if  $f$  is homotopic to a train track map on  $T$  (sends switches to switches, edges to edge paths).

Fix  $f : S \rightarrow S$  a pseudo-Anosov map on a surface  $S$ , along with a pair of measured singular foliations on  $S$  satisfying 2.2 for  $f$ .

**Theorem 3.12** ([Tsa24, Theorem 2.11]). *It is possible to partition the surface above into rectangles such that taking the set of rectangles as a whole, we obtain the tie neighbourhood of some train track  $T$  on  $S$ . The foliations on the surface permeate the rectangles such that for each rectangle, two of its opposing sides lie in stable leaves, and the other two sides lie in unstable leaves. Given a rectangle, the subset of stable leaves in that rectangle form the ties. When the ties of every rectangle are collapsed, we obtain a train track.*

**Corollary 3.13** ([Tsa24, Theorem 2.11]). *The pseudo-Anosov map in the above theorem induces a map on the tie neighbourhood, satisfying the following conditions:*

- Stable sides of rectangles are mapped to stable sides, and similarly for unstable sides.
- Switch ties are mapped to switch ties.
- If  $R_1, R_2$  are rectangles such that  $f(R_1) \cap R_2 \neq \emptyset$ , then  $f(R_1)$  must pass through  $R_2$  completely.
- $f$  induces a train track map on the train track associated to the tie neighbourhood

We emphasize another point, which is crucial for the rest of the article: The transition matrix of the above train-track map is Perron-Frobenius. Furthermore, **its spectral radius is equal to the dilatation of the pseudo-Anosov map that we started with.**

#### 4. PSEUDO-ANOSOV HOMEOMORPHISMS ARISING FROM BRAIDS

**Definition 4.1.** Let  $n \geq 1$ .  $B_n$ , the **braid group on  $n$  strands** is the group with presentation

$$\langle \sigma_1, \dots, \sigma_{n-1} \mid \sigma_i \sigma_{i+1} \sigma_i = \sigma_{i+1} \sigma_i \sigma_{i+1}, \sigma_i \sigma_j = \sigma_j \sigma_i \text{ when } |i - j| \geq 2 \rangle$$

One can visualize elements of  $B_n$  as moves on an  $n$ -strand braid. Draw  $n$  vertical strands, and label their positions  $1, 2, \dots, n$ . Then the generator  $\sigma_i$  swaps the strand in position  $i$  with the strand in position  $i + 1$ , by moving the former under the latter. Note that the strand in position  $i$  is now in position  $i + 1$ , and vice versa. Its inverse  $\sigma_i^{-1}$  also swaps the strand in position  $i$  with the one in position  $i + 1$ , however the former goes *over* the latter instead of under. An example is shown below.

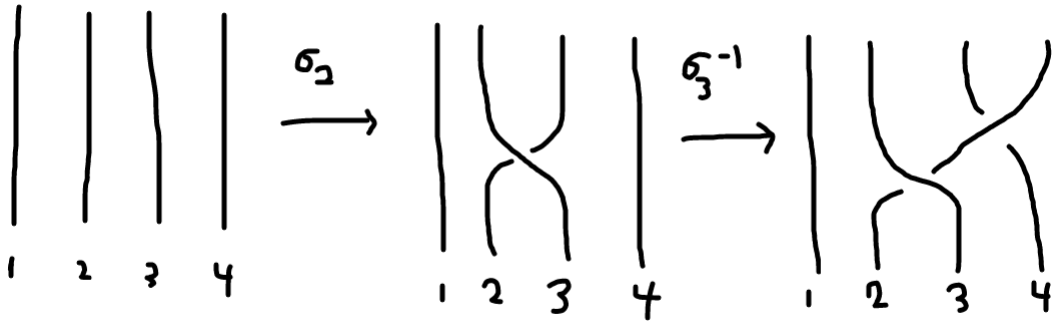


FIGURE 3

Because we can represent braid group elements as moves on a braid, we often refer to such elements simply as "braids". Products of braid moves are also braid moves. We adopt the convention that for an element  $g_1 \dots g_k$ , the rightmost element acts on the braid first. So the element in the above example is  $\sigma_3^{-1} \sigma_2$ . An element of  $B_n$  induces a class of homeomorphisms on  $D_n$ , the  $n$ -punctured disk. Label each puncture from 1 up to  $n$ . The effect of the generator  $\sigma_i$  on  $D_n$  is as follows: let  $U$  be an open ball containing the puncture  $i, i+1$  and no other punctures.  $\sigma_i$  fixes  $\partial U$  while rotating the punctures clockwise so that  $i$  is sent to  $i+1$  and vice versa, as seen below. This is a homeomorphism  $\phi: D_n \rightarrow D_n$ , and the class of homeomorphisms associated to  $\sigma_i$  is the mapping class of  $\phi$ .

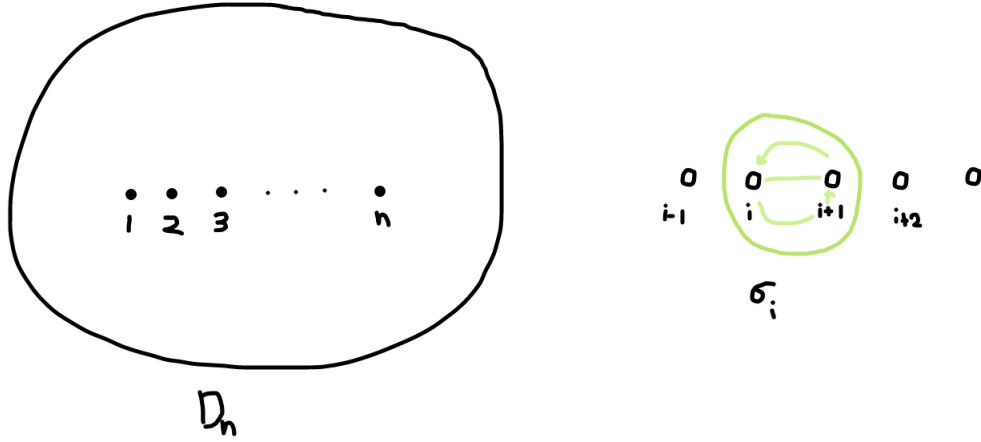


FIGURE 4. A visual example of how braid moves affect an  $n$ -punctured disk. Although the punctures in the disk above lie nicely in a line, generally this is not in the case, as we will see later.

A braid group element is *pseudo-Anosov* if it generates a class of pseudo-Anosov homeomorphisms using the above construction. In [HK06], Hironaka and Kin give two families of braids that are pseudo-Anosov.

**Definition 4.2.** Let  $m, n \geq 1$  be two integers and consider the group  $B_{m+n+1}$ . We define  $\beta_{m,n} \sigma_{m,n} \in B_{m+n+1}$  as the elements which look like the following when drawn out:

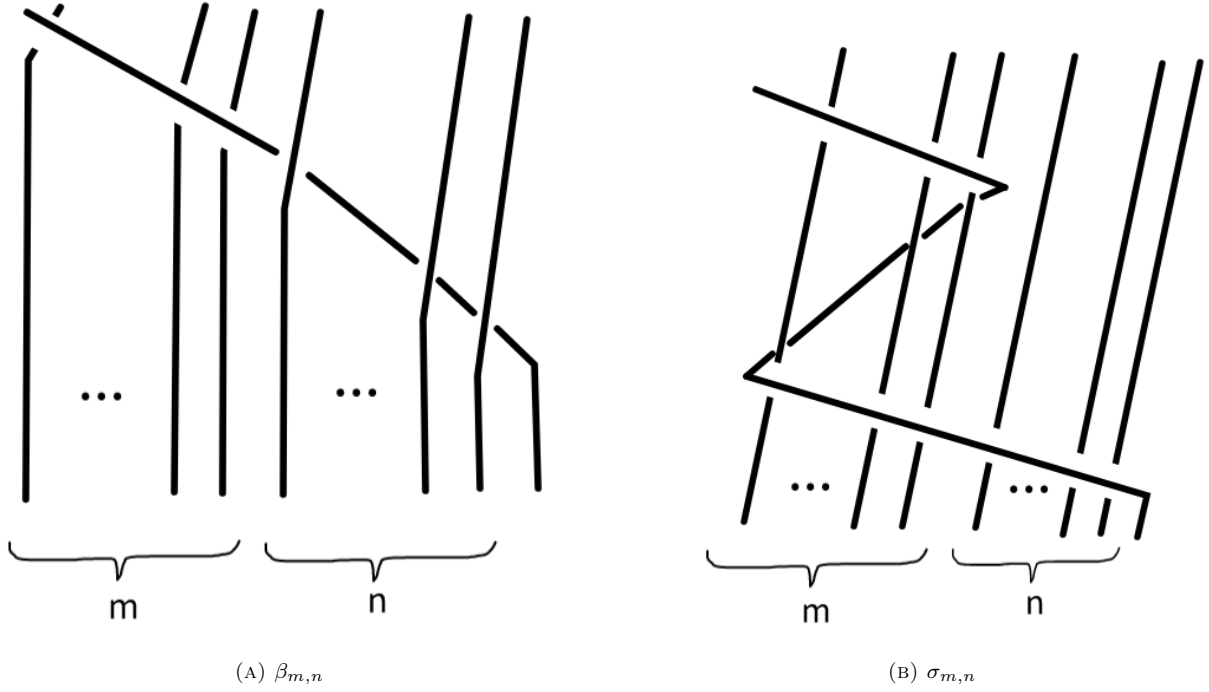


FIGURE 5

## 5. CURVE COMPLEXES

Let  $\Gamma$  be a directed graph.

**Definition 5.1.** A *metric* on  $\Gamma$  is a choice of a positive real number for each edge:

$$m : E(\Gamma) \rightarrow \mathbb{R}_+$$

**Definition 5.2.** A *directed metrized graph* is a directed graph with a metric.

Let  $G$  be an undirected graph with no loops or parallel edges.

**Definition 5.3.** A *weight* on  $G$  is a choice of positive real number for each vertex of  $G$ :

$$w : V(G) \rightarrow \mathbb{R}_+$$

Let  $(G, w)$  be a weighted graph.

**Definition 5.4.** The *clique polynomial* of  $G$  is

$$Q_G(t) = \sum_K (-1)^{|K|} t^{w(K)}$$

where we sum over the cliques  $K$  of  $G$ , and  $w(K) = \sum_{v \in K} w(v)$ . By convention, the empty subgraph is a clique of size 0.

Let there be a directed metrized graph  $\Gamma$ .

**Definition 5.5.** A *simple curve* of  $\Gamma$  is a directed closed path that does not revisit the same vertex of  $\Gamma$  twice.

**Definition 5.6.** The *curve complex* of  $\Gamma$  is an undirected weighted graph that contains information about the simple curves of  $\Gamma$  and whether they meet. For each simple curve  $\gamma$  of  $\Gamma$ , we create a vertex of  $G$  with weight equal to the sum of the metrics of the edges of  $\gamma$ . We join two vertices with an edge if their corresponding simple curves in  $\Gamma$  do not meet at a vertex.

**Theorem 5.7** ([McM15, Theorems 1.2, 1.3]). Let  $(\Gamma, m)$  be a metrized directed graph with the constant metric  $m(e) = 1 \ \forall e \in E(\Gamma)$ . Let  $(G, w)$  be its curve complex. The spectral radius of the adjacency matrix of  $\Gamma$  equals the reciprocal of the smallest positive root of  $Q_G(t)$

**Corollary 5.8** ([McM15, Theorem 1.2]). Let  $f : S \rightarrow S$  be a train track map on  $T \subset S$ . Then the transition matrix  $M$  of  $f$  is the adjacency matrix of some directed graph  $\Gamma$ . Equip  $\Gamma$  with the constant metric  $m(e) = 1$ , and let  $(G, w)$  be the resulting curve complex of  $\Gamma$ . Then  $\lambda(f)$  equals the reciprocal of the smallest positive root of  $Q_G(t)$

## 6. APPLICATIONS OF CURVE COMPLEXES

We apply the methods of [McM15] to calculate the dilatation of pseudo-Anosov maps induced by train track maps from [HK06].

The following figure displays the train track introduced by [HK06] that carries the pseudo-Anosov homeomorphism generated by the braid  $\beta_{m,n}$ , along with the result of the induced train track map on the train track in the second image.

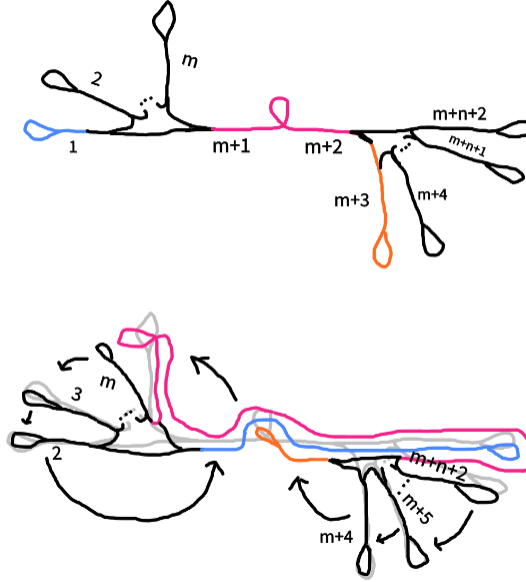


FIGURE 6. Here is a train track that carries the train track map induced by  $\beta_{m,n}$ . The branches have been labeled from 1 to  $m+n+2$ , and a few branches have been colored in order to clarify where they end up under the train track map. There is a puncture singularity in each of the circular shapes.



The transition matrix of the train track map, calculated by looking at the edges, is

$$\begin{array}{cccccccccccc} & 1 & 2 & 3 & \dots & m & m+1 & m+2 & m+3 & m+4 & \dots & m+n+1 & m+n+2 \\ \begin{array}{l} 1 \\ 2 \\ \vdots \\ \vdots \\ m-1 \\ m \\ m+1 \\ m+2 \\ m+3 \\ \vdots \\ \vdots \\ m+n \\ m+n+1 \\ m+n+2 \end{array} & \left[ \begin{array}{l} 0 & 1 & 0 & \dots \\ 0 & 0 & 1 & 0 & \dots \\ \vdots & \vdots & \vdots & & \\ \vdots & \vdots & \vdots & & \\ 0 & 0 & 0 & 0 & 1 & 0 & 0 & \dots \\ 0 & 0 & 0 & 0 & 0 & 1 & 1 & 0 & 0 & \dots \\ 1 & 0 & 0 & 0 & 0 & 0 & 1 & 0 & \dots & \\ 1 & 0 & 0 & 0 & 0 & 0 & 1 & 1 & 0 & \dots \\ 0 & 0 & 0 & 0 & 0 & 0 & 0 & 0 & 1 & 0 & \dots \\ \vdots & \vdots & & & & & & & & & \\ \vdots & \vdots & & & & & & & & & \\ 0 & 0 & 0 & \dots & 0 & 0 & 0 & 0 & 0 & \dots & 1 & 0 \\ 0 & 0 & 0 & \dots & 0 & 0 & 0 & 0 & 0 & \dots & 0 & 1 \\ 1 & 0 & 0 & \dots & 0 & 0 & 2 & 0 & 0 & \dots & 0 & 0 \end{array} \right] \end{array}$$

The directed graph generated by using the transition matrix as an adjacency matrix is the following:

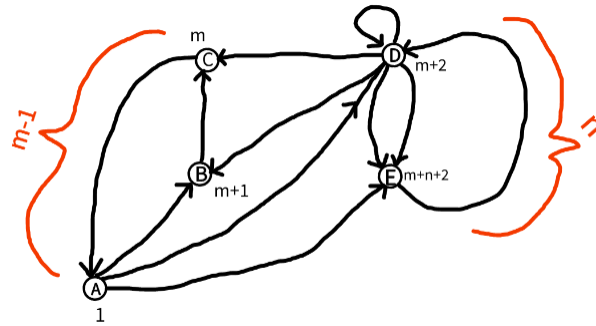


FIGURE 7. Here, all edges have weight 1, except for the two which have their weights labeled using the orange curly brackets. We have added labels for the vertices using the labels for the train track branches that they correspond to.

We tabulate the curves in the directed graph to find the curve complex, shown below:

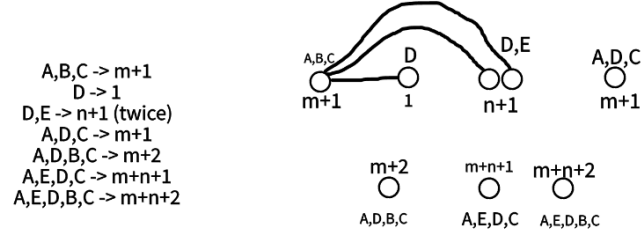


FIGURE 8. Here is the curve complex. Note that the double edge between D and E results in there being two vertices in the curve complex for the curve  $D \rightarrow E \rightarrow D$

The clique polynomial for the case  $n = m + 2$  is:

$$x^{2m+4} - x^{2m+3} - 2x^{m+3} - 2x^{m+1} - x + 1$$

This is reciprocal since

$$\begin{aligned}
 x^{2m+4} & (x^{-2m-4} - x^{-2m-3} - 2x^{-m-3} - 2x^{-m-1} - x^{-1} + 1) \\
 & = 1 - x - 2x^{m+1} - 2x^{m+3} - x^{2m+3} + x^{2m+4}
 \end{aligned}$$

Now we consider  $\sigma_{m,n}$ , the second pseudo-Anosov braid presented in [HK06]. The following figure shows the train track, along with the result of applying the train track map induced by  $\sigma_{m,n}$  on it.

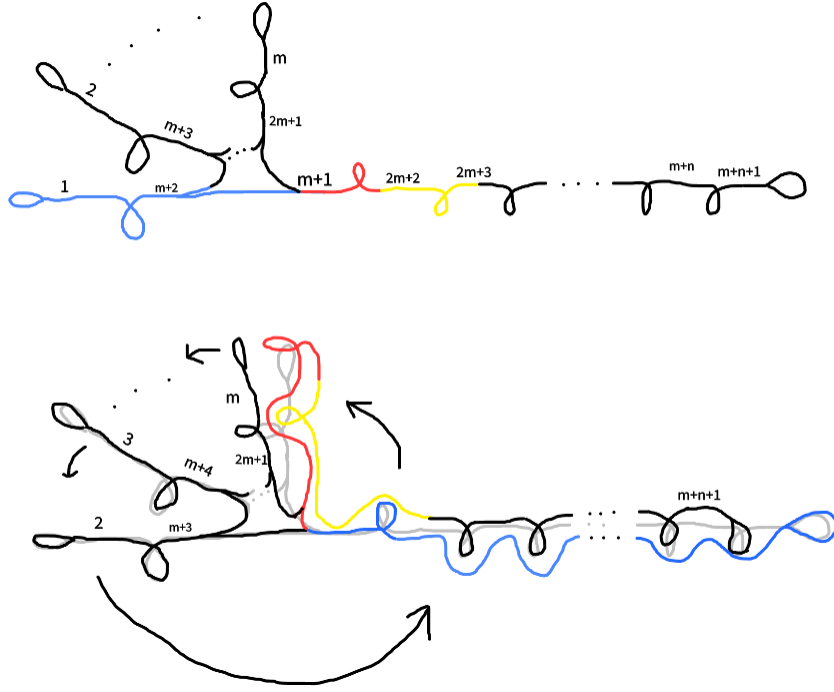


FIGURE 9. The train track is shown on top. The edges have been labeled from 1 to  $m + n + 1$ , and certain subsets of the train track have been colored in order to make it easier when considering the train track map. There exists one puncture singularity in each of the circular shapes. On the bottom, we have the result of the train track map overlayed on the original train track, colored in gray.

[illegible]

Viewing this matrix as the adjacency matrix of a metrized directed graph, we obtain the following graph, which we will take the curve complex of:

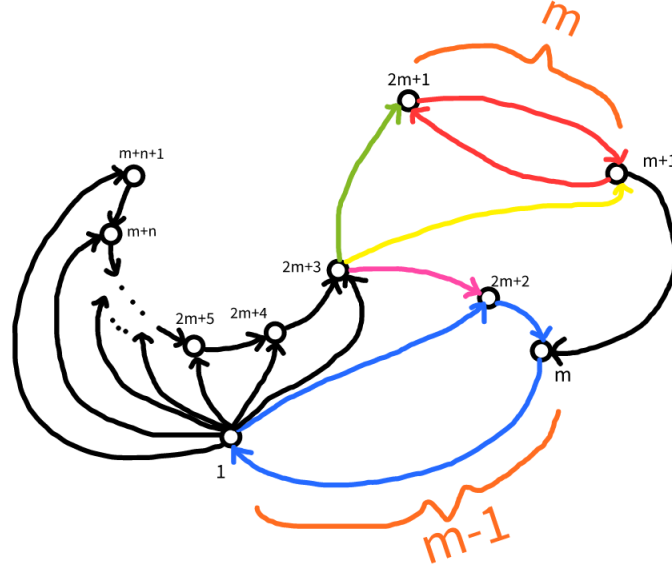


FIGURE 10. Here, we have labeled the vertices of the directed graph according to which branch in the train track they correspond to. The weight of every edge is 1, except for the two edges with weights  $m$  and  $m - 1$ .

And the curve complex:

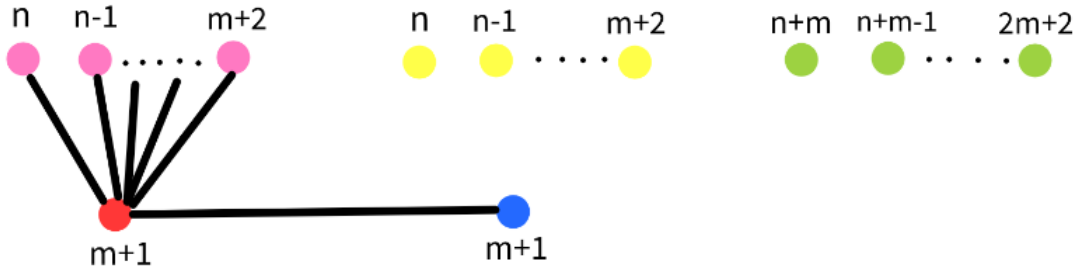


FIGURE 11. Here is the curve complex, with vertex values labeled.

In the case  $n = m + 2$ , the clique polynomial is

$$x^{2m+3} - 2x^{m+2} - 2x^{m+1} + 1$$

This is reciprocal, as

$$\begin{aligned} x^{2m+3}(x^{-2m-3} - 2x^{-m-2} - 2x^{-m-1} + 1) \\ = 1 - 2x^{m+1} - 2x^{m+2} + x^{2m+3} \end{aligned}$$

## 7. ON THE ORIGIN OF CURVES

**7.1. Curves arising from fixed points.** For a fixed point in a train track under a train track map, they are either located inside a  $p$ -pronged singularity, or they are located inside a branch. Furthermore, we distinguish whether they are rotated or not.

**Lemma 7.1.** *Let  $x \in S$  be a fixed point in our train track. Then it is possible to extract one or more cycles in the directed graph arising from this fixed point, depending on whether it is in a  $p$ -pronged singularity or not, and whether it is rotated or not. Furthermore, if it is rotated, we take into account the period of rotation and the number of prongs.*

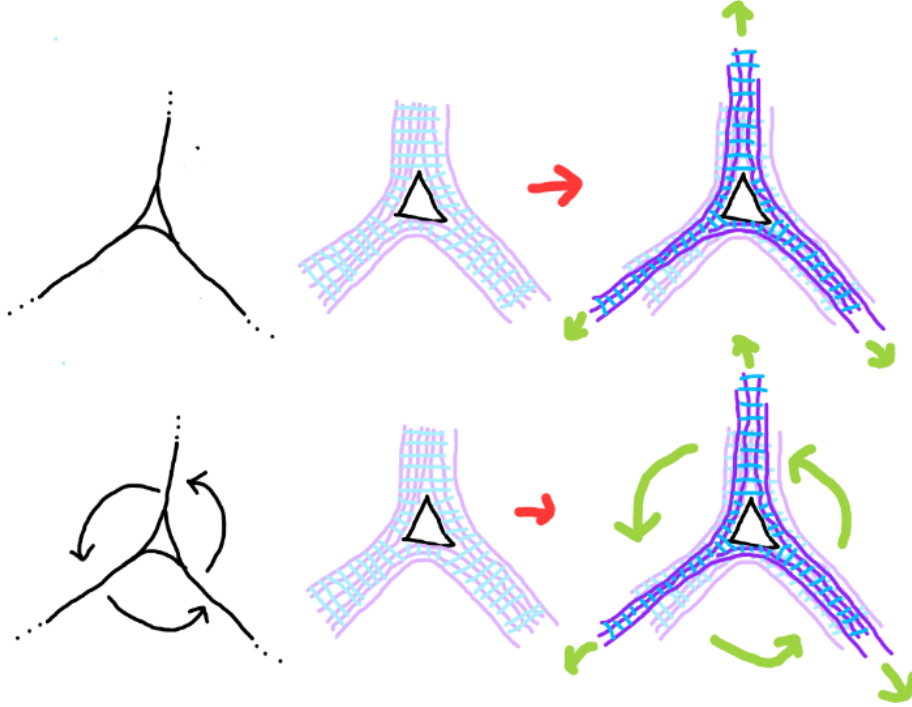


FIGURE 12. Here is a pictorial representation of an example of the first two cases in 7.1 Starting with the train track, we take a Markov partition-tie neighbourhood (middle column). Next, if there is a rotation, we look at the bottom right image. If there is no rotation, we end up in the top right case.

*Proof.* We perform some case analysis.

- **Case 1: Fixed point inside a singularity, non-rotated**

Say the singularity that the fixed point is located in has  $p$  prongs. Since the fixed point is not rotated under the train track map, the prongs are not rotated as well. Labelling the branches associated to the prongs as  $b_1, b_2, \dots, b_n$ , we see that  $D(b_i) = b_i \ \forall i$ . Looking at the tie neighbourhood  $R_i$  associated to each incident branch  $b_i$ , this implies that  $f(R_i)$  passes through  $R_i$  at least once. Hence we obtain at least one loop rooted at  $v_{b_i}$  for each  $b_i$ , where  $v_{b_i}$  is the vertex in the directed graph corresponding to the branch  $b_i$ .

So for a non-rotated fixed point inside a  $p$ -pronged singularity, we obtain  $p$  length-1 curves in the directed graph.

- **Case 2: Fixed point inside a rotated singularity**

Let there be  $p$  prongs and let the period of rotation be  $n$ .  $n$  must divide  $p$ . We may take a Markov partition-tie neighbourhood of our train track, then apply the train track map  $n$  times. Similar to the first case, the unstable sides expand. This time, there is also a rotation. Thus, we end up with  $\frac{p}{n}$  cycles in the directed graph, each of length  $n$ .

- **Case 3: Fixed point inside a branch (rotated or unrotated)** In this case, since the point inside the branch is fixed, the train track map must send the branch into itself; Hence we obtain a self-loop at the vertex in the directed graph corresponding to the branch containing the fixed point.

□

**7.2. Curves arising from boundary rotations.** Given a train track  $T$  on a disk  $D$ , we denote a cusp to be *boundary facing* if there exists a continuous path from the cusp to  $\partial D$  without crossing  $T$ .



FIGURE 13. We give an example of a boundary facing (left) and a non-boundary facing cusp (right)

**7.2.1. Where cusps end up during a train track map.** A subtle point is where cusps ultimately move to after a train track map. Sometimes, it is not enough to look at where neighbouring edges of a cusp are sent to in order to deduce where the cusp is sent to; It could also be necessary to make edge identifications which propel the cusp to another location on the train track. We provide an example in the following figure, showing a train track immediately following a map, plus the edge identifications that propel the cusp in blue to its final location:

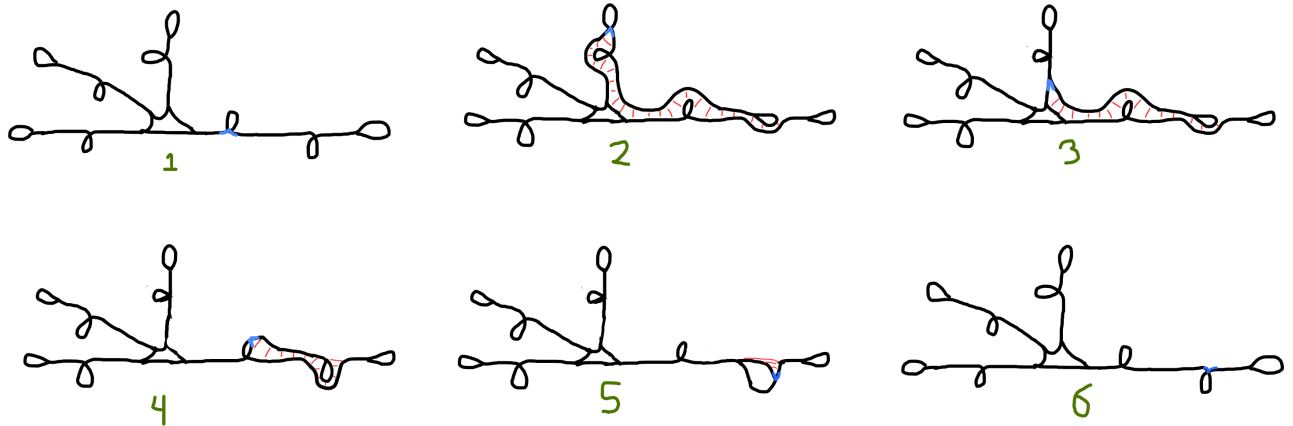


FIGURE 14

### 7.2.2. Boundary rotations.

**Definition 7.2.** Given a train track  $T$  and a train track map  $f : S \rightarrow S$ , we label the boundary-facing cusps of  $T$  as  $c_1, \dots, c_n$ . Taking into account the subtle point in the previous section, if  $f$  sends  $c_i$  to  $c_{i+1}$  and  $c_n$  to  $c_1$  we say that  $f$  exhibits a **boundary rotation** on  $T$ .

**Definition 7.3.** Given a train track on a surface  $S$  and cusps  $c_1, c_2$  on  $S$  that appear in consecutive order when moving around the perimeter of the train track, the **outer boundary path** from  $c_1$  to  $c_2$  consists of the rectangles passed if one follows a path from  $c_1$  to  $c_2$ , going around the outer boundary. See the figure below.

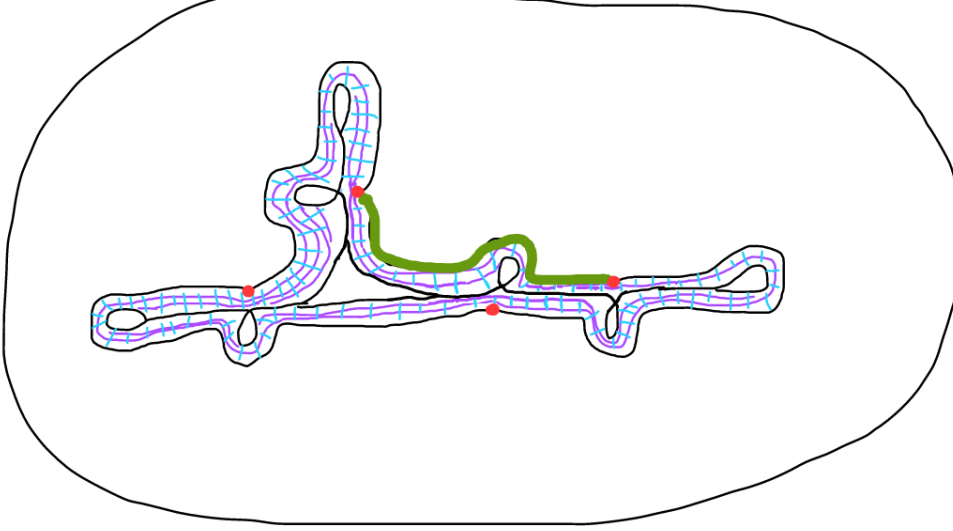


FIGURE 15. Here, the thickened green line bounds the outer boundary path between two consecutive cusps. The cusps are marked in red.

**Lemma 7.4.** In a boundary rotation of period  $n$ , it is possible to extract a cycle in the directed graph of length  $n$ .

*Proof.* The first steps we take are illustrated below with an example train track.

- (1) This is our starting train track on a disk. Punctures are marked by black dots, cusps are marked by red dots (for illustration purposes only)
- (2) First, we thicken the train track into a Markov partition-tie neighbourhood.
- (3) Then, we cut out the edges of the train track (including the punctures), leaving behind just the thickened Markov partition on the disk.
- (4) Next, we perform the operation of collapsing the outer boundary to a single point and turning the cut-out region inside-out, which results in our rectangles now belonging on a punctured sphere. The boundary of the disk in (3) (highlighted in black) is now a puncture in the disk (the black dots in (4) - (6) )
- (5) We homotope the tie neighbourhood for visual purposes
- (6) Here, we show the effect of the induced train-track map on the sphere. By assumption we have a boundary rotation, so the cusps (in red) are rotated around 90 degrees here. The surrounding tie neighbourhoods also rotate 90 degrees. The stable foliations contract while the unstable ones dilate, leading to the new train track (drawn using darker shades, and overlayed on the old train track).



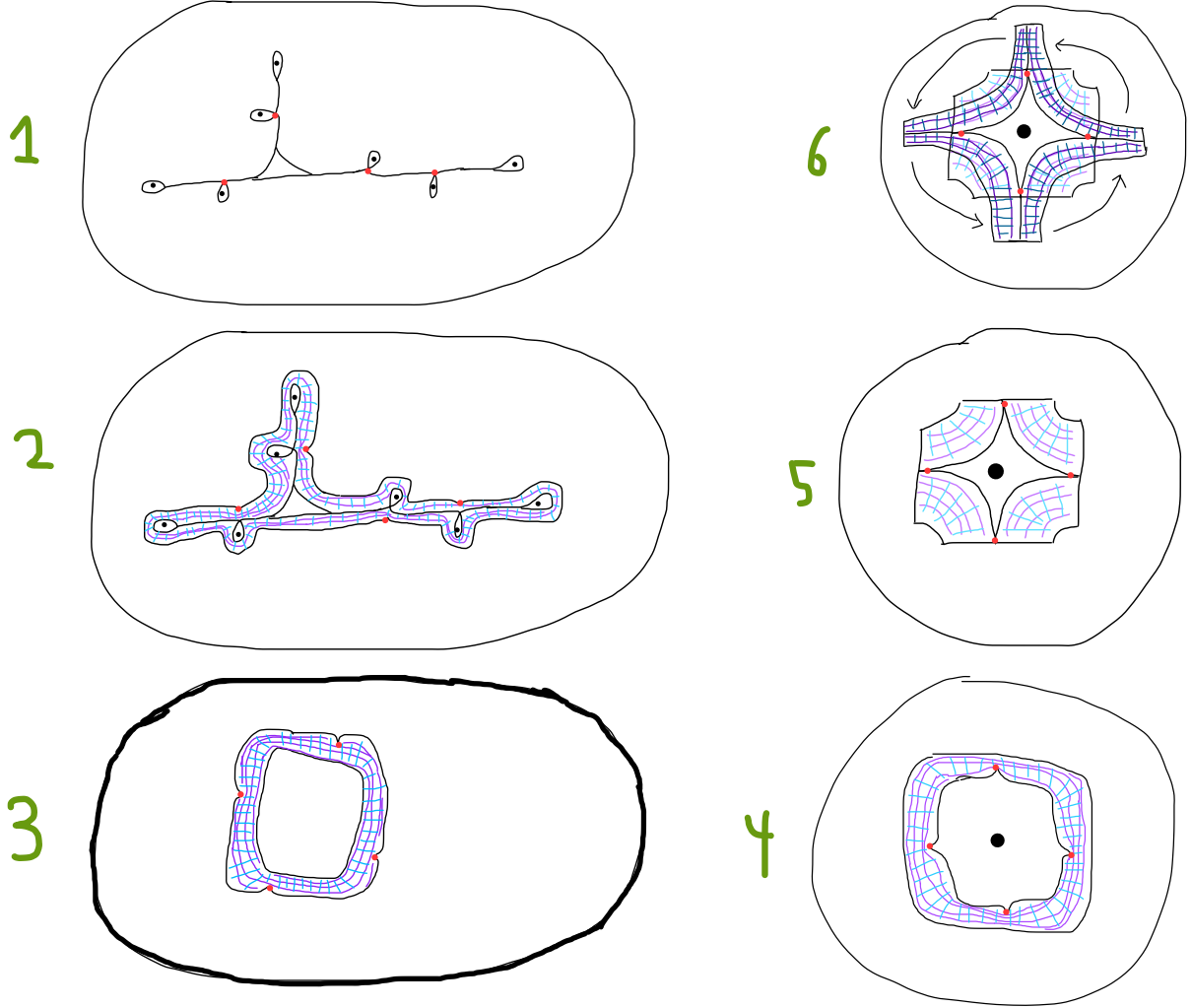


FIGURE 16

This shows that the image of the outer edge path from the cusp  $c_i$  to  $c_{i+1}$  contains the outer edge path from the cusp  $c_{i+1}$  to  $c_{i+2}$ , for each cusp  $c_i$ . We introduce some temporary notation. For  $i \in \{1, 2, \dots, n\}$ , let  $P_i$  denote the rectangles comprising the outer boundary path from the  $i^{th}$  to the  $i+1^{th}$  cusp. For  $i = n$ , these are the rectangles going from the  $n^{th}$  to the  $1^{st}$  cusp. As shown earlier in the lemma, we have  $f(P_i) \supset P_{i+1}$ . Next, we define subsets  $\{Q_i\}$  of the train track-tie neighbourhood inductively as follows: Let  $Q_n \subset P_n$  be the subset that satisfies  $f(Q_n) = P_1$ . Next, for  $i = 1, \dots, n-1$ , define  $Q_i \subset P_i$  to be the subset that satisfies  $f(Q_i) = Q_{i+1}$ . It is always possible to find such a subset since  $f(P_i) \supset P_{i+1} \supset Q_{i+1}$ . Furthermore each  $Q_i$  is a contiguous segment of rectangles, since  $f$  is continuous, so the preimage of  $P_i$  (which is connected) is connected. Hence we have

$$f(Q_1) = Q_2, f^2(Q_1) = Q_3, \dots, f^{n-1}(Q_1) = Q_n, \supset Q_1$$

Since  $f$  is a train track map on the level of tie neighbourhoods, it is invertible. So we have

$$f^{-n}(P_1) = Q_1 \subset P_1$$

By Brouwer's fixed point theorem, there exists an  $x \in Q_1 \subset P_1$  such that  $f^{-n}(x) = x$ , which implies  $f^n(x) = x$ . This fixed point of  $f^n$  is a periodic point of period  $n$  of  $f$ , and it allows us to extract a cycle of period  $n$  from the directed graph as follows: Take the rectangle initially containing  $x$  as  $R_1$ , and consider  $e_1$ , the vertex in the directed graph corresponding to  $R_1$ . Applying  $f$ , we see that  $x$  is mapped to a second rectangle,  $R_2$ . Now since  $x \in R_1$ , this implies that  $f(R_1)$  passes through  $R_2$ . So if  $e_2$  is the vertex corresponding to  $R_2$ , then there is an edge going from  $e_1$  to  $e_2$  in the directed graph. Repeating this process until  $x$  is mapped back to itself after  $n$  iterations of the map  $f$  yields a cycle in the directed graph of period  $n$ :

$$e_1 \rightarrow e_2 \rightarrow \dots \rightarrow e_{n-1} \rightarrow e_n \rightarrow e_1$$

□

**7.3. Curves arising from puncture cycles.** Our train track may contain punctures, which are one-pronged singularities. Note that each puncture may have multiple branches coming out of it, as shown below:



FIGURE 17

**Definition 7.5.** A *puncture cycle* is a sequence of punctures  $p_1, p_2, \dots, p_n$  such that  $f(p_i) = p_{i+1}$ ,  $f(p_n) = p_1$ . In the train tracks that we will be working with, each puncture is enclosed by an edge that ends at a cusp, called the *imaginary edge*. Furthermore, we require that the edges different from the surrounding edge, denoted the *real edges*, satisfy the following: If  $f(p_i) = p_{i+1}$ , then the derivative of each real edge of  $p_i$  is a real edge of  $p_{i+1}$ , and the imaginary edge of  $p_i$  is sent to exactly the imaginary edge of  $p_{i+1}$ . See below for an example.

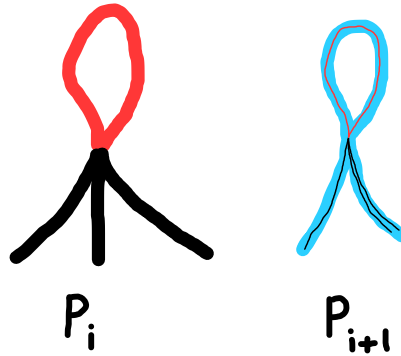


FIGURE 18. Here, we have two punctures along with the surrounding edges in the train track. The real edges of  $p_i$  pass through the real edges of  $p_{i+1}$  first. The second puncture's surrounding edges have been colored blue in order to make apparent where the edges of  $p_i$  are being sent to, and the train tracks have been thickened for visual clarity.

**Remark 7.6.** *The real and imaginary edges mentioned above are part of a more general definition, but we will not discuss it here. See [HK06] for a discussion.*

Our goal is to extract one curve from each puncture cycle in our train track map.

**Lemma 7.7.** *Given a puncture cycle, we may extract a cycle in the directed graph of the same period*

*Proof.* Let  $p_1, \dots, p_n$  be punctures in the train track  $S$  such that the train track map  $f : S \rightarrow S$  satisfies  $f(p_i) = p_{i+1}$ ,  $f(p_n) = p_1$ . We take a Markov partition that is a tie neighbourhood of the train track. Letting  $s_i$  denote the switch tie of  $p_i$ , we have that  $f(s_i) \subset s_{i+1}$  by the definition of a train track map, since they must map switch ties to switch ties.

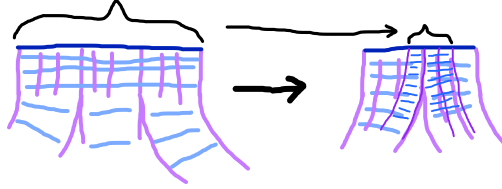


FIGURE 19. We take a Markov partition-tie neighbourhood of the train track, and look at the train track map while focusing on the part in the previous figure that is below the respective switch ties of each puncture. The purple lines are the unstable foliations, while the light blue lines are the stable ones. The dark blue lines are the switch ties. Note that since the train track map is continuous, the image of the switch tie of the left puncture is connected (emphasized using curly brackets). The image of the train track on the left is shown on the right by using thinner lines and darker shades of purple and blue.

We assume the switch tie is part of a stable foliation by convention. Iterating this, we see that  $f^n(s_i) \subsetneq s_i$  (a train track map raised to a positive power is still a train track map). Taking  $i = 1$  and using the Brouwer fixed point theorem, we see that  $\exists x_0 \in f^n(s_1) \subset s_1$  such that  $f^n(x_0) = x_0$ .

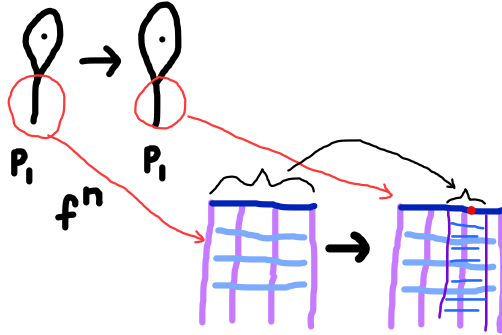


FIGURE 20. Here is the scenario described above.  $p_1$ 's incident branches are mapped to itself under  $f^n$  (there is only one branch in the illustration). Looking at the Markov partition/tie neighbourhood on the other side of the switch tie, we see that  $f^n$  contracts the rectangle of the branch into itself. In particular the stable switch tie is contracted into itself. So by Brouwer's fixed point theorem, there is a fixed point  $x_0$  of  $f^n$  (labeled as a red dot). It is also a periodic point of  $f$

Since each switch tie of a puncture is partitioned into the widths of rectangles incident to the puncture, each point on the switch tie lies in exactly one of the rectangles. For  $x \in s_i$ , let  $R(x)$  denote the rectangle whose side contains  $x$ . Then we extract a sequence of rectangles  $R(x_0), R(f(x_0)), R(f^2(x_0)), \dots, R(f^{n-1}(x_0))$ . By construction, we have that  $f(R(f^i(x_0)))$  passes through  $R(f^{i+1}(x_0))$ . Thus the vertices in the directed graph corresponding to  $R(x_0), R(f(x_0)), R(f^2(x_0)), \dots, R(f^{n-1}(x_0))$  form a cycle of length  $n$ .

Since  $f$  is a continuous map, if  $b_i$  is a branch incident to  $p_i$ , then  $f(b_i)$  will be incident, or pass through  $p_{i+1}$ . On the level of the Markov partition, this means that each rectangle incident to the puncture  $p_i$  passes through at least one of the rectangles incident to  $p_{i+1}$ .  $\square$

**Lemma 7.8.** *Cycles in the directed graph arising from puncture cycles cannot intersect at a vertex more than twice.*

*Proof.* Following the construction in the previous lemma, we see that by inflating the train tracks into a Markov partition, there will be a periodic point on the switch tie of each puncture in the puncture cycle.

Let  $w$  be a vertex in the directed graph such that there exist distinct subpaths of cycles that come from puncture cycles,  $v_1 \rightarrow w$  and  $v_2 \rightarrow w$ . It is possible that they are different subpaths of the same cycle. Consider  $e_w$ , the edge in the train track corresponding to the vertex  $w$ . We use the same notation for the other vertices. The existence of the subpath  $v_1 \rightarrow w$  implies that  $f(e_{v_1})$  passes through  $e_w$ . In fact, more is true. For example, since  $v_1 \rightarrow w$  comes from a puncture cycle, there must be at least one periodic point on one of the two stable sides of  $e_{v_1}$ , and similarly for  $e_{v_2}$ .

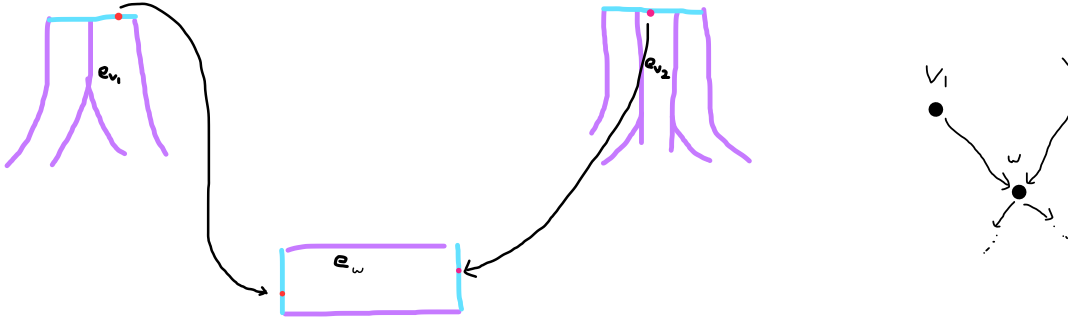


FIGURE 21. Here is the situation described in the previous paragraph. Note the choice of number of branches was chosen arbitrarily for the illustration. The periodic points arising from the argument in 7.7 are marked in red.

When the train track map maps  $e_{v_1}$  to  $e_w$ , this periodic point is mapped to a stable side of the rectangle  $e_w$ . Similarly, the periodic point on a stable side of  $e_{v_2}$  is mapped to a stable side of  $e_w$ . Since each rectangle has at most two stable sides, each side is the leaf of the stable foliation, and there can be at most one periodic point on a leaf, this implies that the stable sides of each rectangle can have at most 2 periodic points in total. This implies that cycle(s) in the directed graph coming from puncture cycles cannot intersect at a vertex more than twice.  $\square$

**Lemma 7.9.** *Given two distinct puncture cycles, it is possible to extract two distinct cycles in the directed graph arising from them*

*Proof.* Let  $f : S \rightarrow S$  be the train track map, and assume the contrary. This means that two distinct puncture cycles give rise to the same cycle in the directed graph. Let  $p_1, \dots, p_n$  be the punctures of one cycle and  $q_1, \dots, q_n$  be the punctures of the other. Following 7.7, we take a Markov partition-tie neighbourhood of the train track and

locate the periodic points on the switch ties of  $\{p_i\}$  and  $\{q_i\}$ . Since the two puncture cycles give rise to the same directed graph cycle, this implies the existence of rectangles  $R_1, \dots, R_n$ , where  $R_i$  contains the periodic points on the switch ties of  $p_i$  and  $q_i$ . Of the two stable sides of each  $R_i$ , one is a subset of the switch tie of  $p_i$ , and the other is a subset of the switch tie of  $q_i$ . We take arbitrarily one of the rectangles, say  $R_1$ . It is depicted below.



FIGURE 22. Here is  $R_1$ . The stable side is in blue and the unstable side is in purple. The foliations are not drawn for clarity, and the periodic points on the stable sides (one from each puncture cycle) are labeled in red.

We consider the image of  $R_1$  after  $n$  iterations of the train track map,  $f^n$ , where  $n$  is the period of the two puncture cycles. Since the periodic points are of period  $n$ , they become fixed points under  $f^n$ . Furthermore, by the definition of the puncture cycle, the derivatives of the real edges incident to  $p_1$  under  $f$  must be the real edges of  $p_2$ . Iterating this  $n$  times, we see that the derivatives of each real edges of  $p_1$ , in particular  $R_1$ , is another real edge of  $p_1$ , and similarly for  $q_1$ . We have abused notation a bit and referred to edges as rectangles, but the correspondence under the Markov partition-tie neighbourhood construction is clear. However, due to the presence of the fixed points on the stable sides of  $R_1$ , and by the definition of the puncture cycle, we know that the derivative of  $R_1$  under  $f^n$  equals  $R_1$ , picking either stable side of the rectangle as the front. However, to reconcile that fact with the elongation of the unstable side of the rectangle, and that unstable foliations must be sent to unstable foliations, it is necessary that under  $f^n$ ,  $R_1$  must pass through itself more than once.

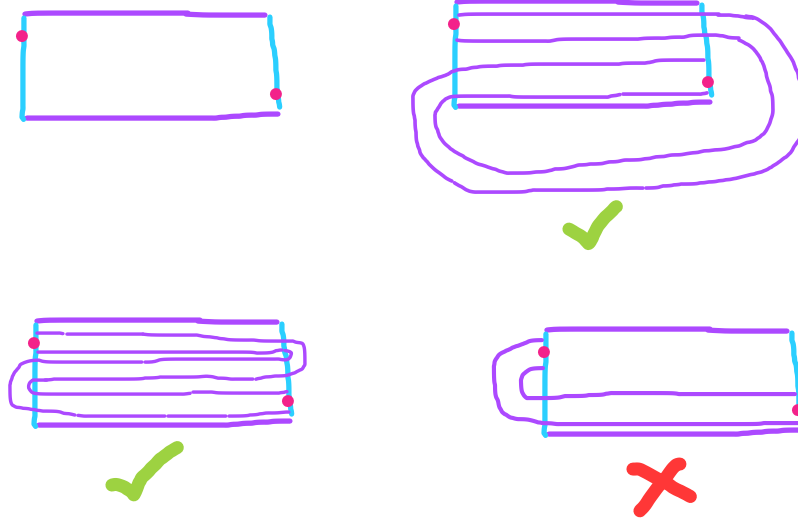


FIGURE 23. Here is an example of the above discussion. On the top left is  $R_1$ , depicted with the fixed points of  $f^n$  on its stable sides. The top right and bottom left depict possibilities of what  $f^n(R_1)$  might look like, overlayed on top of  $R_1$ . Note that the fixed points are sent to themselves. The part of  $f^n(R_1)$  drawn outside  $R_1$  is only an abstract depiction. On the bottom right we have an invalid scenario of  $f^n(R_1)$ ; Such a location of  $f^n(R_1)$  in relation to  $R_1$  is forbidden because taking the derivative of  $f^n$  of  $R_1$ , with the left side as the front, does not yield back  $R_1$ .

Since  $R_1$  is sent to itself at least twice under  $f^n$ , this implies that in the directed graph cycle that is procured by both the puncture cycles, there is a double edge somewhere. That implies that it is possible to extract distinct cycles in the directed graph from the two puncture cycles.

□

**Lemma 7.10.** *Given  $n$  puncture cycles, it is possible to extract at least  $n$  curves in the directed graph arising from those puncture cycles*

*Proof.* We prove the following statement, which implies the lemma:

The intersection of two cycles in the directed graph that arise from puncture cycles cannot contain a closed curve.

This implies the lemma; Given  $n$  puncture cycles, they must each give rise to a cycle in the directed graph. Since any pair of such cycles do not both contain the same curve, it is possible to choose a distinct curve for each cycle.

First, let  $C_1$  and  $C_2$  be two cycles in the directed graph that arise from puncture cycles, and assume they both contain some closed curve  $C$  with  $n$  vertices. We consider an arbitrary vertex  $v$  in  $C$ . This corresponds to a branch in the train track which belongs to the periodic cycle of branches (see 7.7) associated to the two puncture cycles from which  $C_1$  and  $C_2$  originate. Thus, after inflating the train track to a Markov partition-tie neighbourhood, this rectangle contains one periodic point on each of its two stable sides, one corresponding to  $C_1$  and the other to  $C_2$ . After iterating the train track map  $n$  times, the rectangle is sent back to itself, and for the same reason as in the last paragraph of 7.9, it must be sent to itself more than once. That implies the existence of multiple edges between  $v_1, v_2 \in C$  in the overlapped curve, meaning that  $C_1$  and  $C_2$  run along different edges out of the ones going between  $v_1$  and  $v_2$ . Hence  $C_1$  and  $C_2$  do not completely overlap in the curve  $C$ .

□

**Lemma 7.11.** *A puncture cycle and a fixed point-singularity rotation in the train track cannot lead to the same cycle in the directed graph*

*Proof.* Assume the contrary. Then there is a rotated fixed point  $x \in S$ , our surface of our train track map  $f$  such that the branches incident to the fixed point are mapped to each other and result in a cycle in the directed graph. Since this cycle is also the result of a puncture cycle, necessarily we have that the other ends of the said branches are punctures. We inflate our train track into a Markov partition-tie neighbourhood and apply the train track map. On each rectangle corresponding to a branch incident to the fixed point, there must be one periodic point on each of the two stable sides: one coming from the rotated fixed point and one coming from the puncture cycle. Then by the same reasoning as 7.9, there has to be a double edge somewhere along the cycle, resulting in it being possible to extract two distinct cycles in the directed graph, one for the fixed point rotation and one for the puncture cycle.

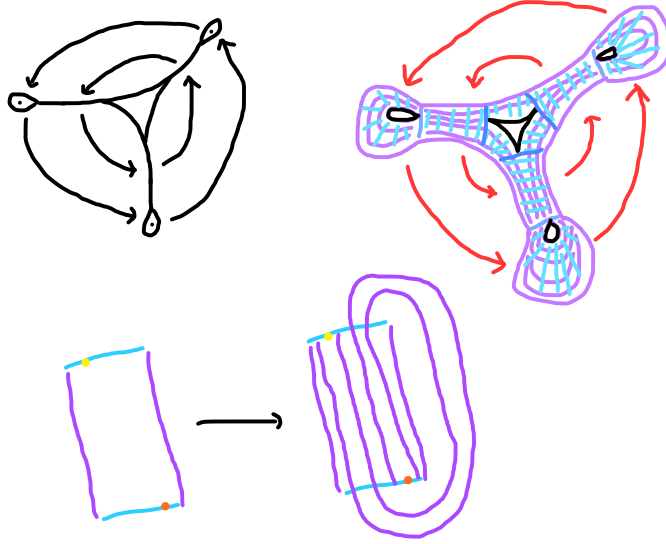


FIGURE 24. An example of the scenario above. Here, on each rectangle incident to the fixed point, there are two fixed points, one on each stable side.

□

## 8. THE MINIMUM NUMBER OF FIXED POINTS

**8.1. Lefschetz's fixed point theorem.** Lefschetz's fixed point theorem allows one to lower-bound the number of fixed points of a homeomorphism by observing the induced map on the homology groups. We can apply this theorem to train track maps to assure the existence of a certain quantity of fixed points in the train track. This is beneficial towards the goal of raising the lower bound on the dilatation of a pseudo-Anosov map. The more fixed points there are in the train track, the more curves there will be in the corresponding directed graph, due to the computations made in 7.1. This increases the number of vertices in the curve complex, which will decrease the minimum positive root of the curve complex's clique polynomial. This follows because if  $H \subset G$  is a subgraph of the curve complex, then  $\lambda(H) \leq \lambda(G)$ , where  $\lambda(G)$  is the reciprocal of the minimal positive root of the clique

polynomial of  $G$  [McM15, page 196]. Since the dilatation of the train track map is the reciprocal of the minimum positive root, the upshot is that *the minimum possible dilatation will increase if we can demonstrate the existence of more fixed points.*

We also restrict the number of prongs that singularities may have using a version of the Poincaré-Hopf theorem. This further restriction is also discussed below.

**8.2. Applying the theorem.** In our case where we are dealing with train track maps on a punctured disk, the Lefschetz fixed point theorem condenses to the following statement:

**Theorem 8.1** (Lefschetz fixed point theorem, special case). *Let  $f : S \rightarrow S$  be a train track map on a (possibly punctured) disk or 2-sphere  $S$ .*

*Then, we have*

$$\sum_{x \text{ is a fixed point of } f} \text{ind}_{Lef}(x) = 2$$

*Where, when  $x$  is a  $p$ -pronged singularity, we have*

$$\text{ind}_{Lef}(x) = \begin{cases} -p + 1 & x \text{ is unrotated} \\ 1 & x \text{ is rotated} \end{cases}$$

*Note that in some cases, such as when there is a boundary rotation, we collapse the disk into a sphere and consider the induced train track map  $\tilde{f}$  on the sphere.*

The second restriction we place is a variant of the Poincaré-Hopf theorem for train track maps. However, we now place restrictions on the singularities, not the fixed points. We place conditions on the number of prongs that singularities (e.g. punctures) in the train track can have. It is delineated below:

**Theorem 8.2** (Poincaré-Hopf, special case). *Let  $f : S \rightarrow S$  be a train track map on a surface  $S$ . Then*

$$\sum_{x \text{ is a singularity}} \text{ind}_{P-H}(x) = \chi(S)$$

*where*

$$\text{ind}_{P-H}(x) = \begin{cases} -\frac{p-2}{2} & x \text{ is a } p\text{-pronged non-punctured singularity} \\ -\frac{p}{2} & x \text{ is a } p\text{-pronged punctured singularity} \end{cases}$$

*and  $\chi(S)$  is the Euler characteristic. In particular,  $\chi(S) = 1 - n$  when  $S$  is an  $n$ -punctured disk and  $\chi(S) = 2 - n$  when  $S$  is an  $n$ -punctured sphere.*

These theorems imply that the set of fixed points is always nonempty. For a given train track map on an  $n$ -punctured disk, we may consider the possible configurations of the fixed points (i.e. whether each one is rotated or unrotated) such that each configuration satisfies the above theorems. Next, out of those valid configurations, we find which one leads to the minimum dilatation of the train track map. This is the worst-case scenario (since we are trying to *raise* the lower bound, so we hope that this minimum is higher than the current lower bound) and provides a lower bound on the dilatation under the conditions that we stated. More careful and precise reasoning can improve the bound.



**8.3. Example.** Consider the following example: Let there be a train track with  $n$  punctures on a disk  $S$ . Say the train track map  $f : S \rightarrow S$  has a boundary rotation with period  $q \geq 1$ . Say we also know that there is a rotated fixed point of some unknown number of prongs  $p \geq 1$ . Furthermore, say that the  $n$  punctures lie in a single orbit. This is a reasonable assumption to make, since in general, the fewer number of puncture orbits, the fewer the number of vertices in the curve complex and the lower the resulting dilatation. We wish to determine a lower bound on the dilatation of this train track map.

First, we collapse the boundary so that we are now working on an  $n$ -punctured sphere. The boundary rotation has turned into a  $q$ -pronged *unpunctured* rotated singularity, where  $q \geq 1$  is the number of boundary facing cusps.

We do not need to worry about the Lefschetz fixed point theorem because it is automatically satisfied in this case. On the sphere, the rotated fixed point coming from the outer boundary and the other rotated fixed point assumed to already exist on the disk each contribute a Lefschetz index of 1 to the sum in the theorem's formula. There are no other fixed points, hence the theorem is satisfied. From the Poincare-Hopf theorem, we obtain

$$\begin{aligned} \sum_{x \text{ is a singularity}} \text{ind}_{P-H}(x) &= \chi(S) = 2 - n \\ &= -\frac{1}{2} \cdot n - \frac{p-2}{2} - \frac{q-2}{2} = 2 - n \end{aligned}$$

Where

- The first term is coming from the  $n$  punctures
- The second term is coming from the unpunctured fixed point singularity with  $p$  prongs
- The third term is coming from the unpunctured rotated outer boundary singularity that was created when we collapsed to a sphere.

From this relation, we obtain

$$n = p + q$$

We make the assumption that the cycles in the directed graph induced by the fixed points and puncture cycles above are curves. Furthermore, we make the assumption that the induced curves of the boundary rotation and the fixed point meet at a vertex somewhere in the train track. This is also a reasonable assumption to make: There are only  $n$  edges in our train track because it is a tree if we count the punctured singularities as vertices, of which there are  $n + 1$  ( $n$  from the punctures, 1 from the fixed point; The outer boundary does not contribute despite counting as a singularity since it is disconnected from the train track). Since  $p + q = n$ , the puncture cycle meets the other two cycles described above at vertices, keeping in mind that we assumed the puncture cycle induces a curve in the directed graph. Furthermore, we would expect most of the time for the  $p$  edges of the fixed point cycle and the  $q$  edges of the boundary rotation cycle to meet somewhere, since there are only  $n$  edges in total. Hence, following these assumptions, we obtain in the curve complex a vertex of weight  $n$ , a vertex of weight  $p$ , and a vertex of weight  $q$ . Under these assumptions, there are no edges in the curve complex, since for any two curves, there is a vertex in the directed graph where they meet.

So we obtain a clique polynomial of

$$1 - t^n - t^q - t^p$$

We find it more informative to study  $\lambda^n$ , the resulting dilatation raised to the power of the number of punctures. This will give us information about how  $\lambda$  evolves asymptotically as  $n \rightarrow \infty$ . We consider the new equation

$$1 - t - t^{\frac{q}{n}} - t^{\frac{p}{n}}$$

The roots of this new equation are precisely the roots of the previous equation raised to a power of  $n$ : If  $\alpha$  is a root of this new equation, then we see that  $\alpha^{\frac{1}{n}}$  is a root of the previous equation. We see that for all values of  $n$ ,

the smallest positive root is maximized when  $p = q$ . Furthermore, the value of this root is held constant if  $p = q$  and we vary  $n$ . We see that its value is

$$\left(\frac{-2 + \sqrt{8}}{2}\right)^2$$

We see that the resulting dilatation value is  $\frac{1}{\left(\frac{-2 + \sqrt{8}}{2}\right)^2} = \left(\frac{2 + \sqrt{8}}{2}\right)^2 \approx 5.8284$ . Hence our asymptotic lower bound for the dilatation is

$$\lambda^n \geq 5.8284(\text{approximately})$$

This applies for all train track maps satisfying the conditions we assumed in the example. This process shows the skeleton of how one might apply the Poincare-Hopf and Lefschetz theorems to raise the lower bound of the dilatation. Refinements of the argument in this example can lead to stronger bounds for more general situations.

#### APPENDIX A. DIRECTED GRAPH CURVES FROM HIRONAKA AND KIN

We determine the provenance of the directed graph curves from the  $\beta_{m,n}$  and  $\sigma_{m,n}$  families from [HK06].

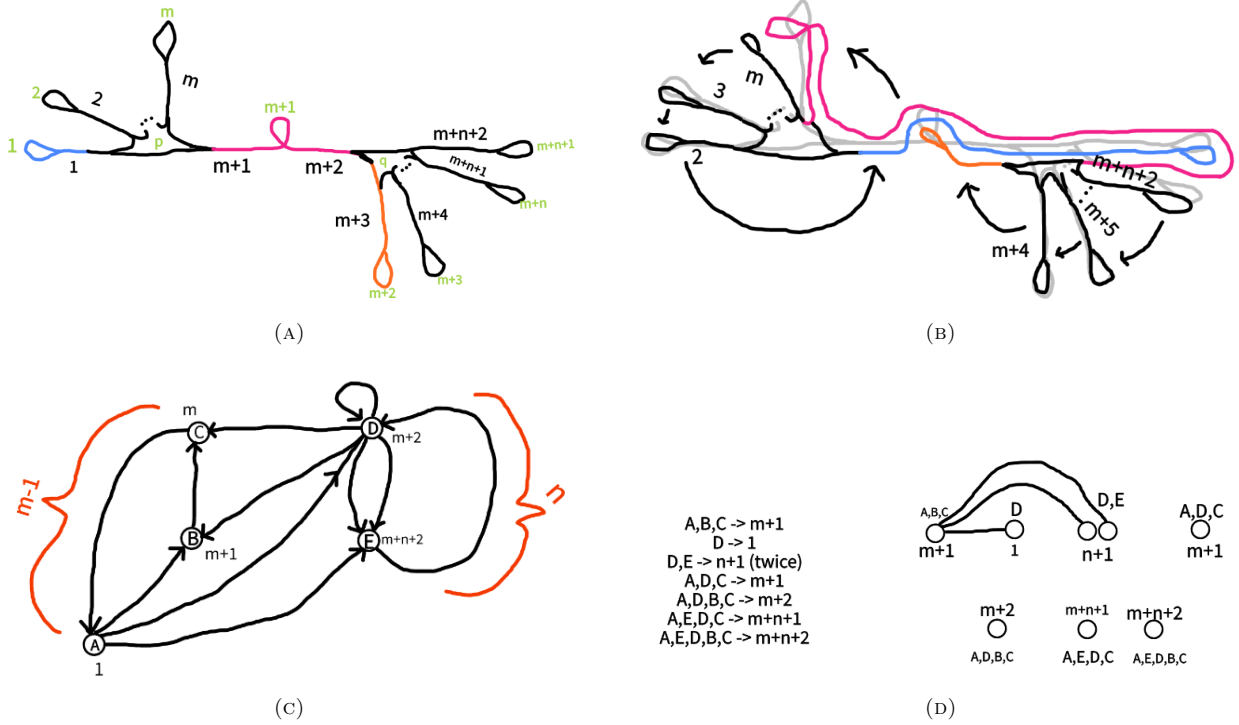


FIGURE 25. We reproduce here the relevant figures. The punctures in the train track figure have been given labels which match the labels in [HK06]

We note how some vertices in the curve complex arises, i.e. where each curve in the directed graph comes from.

- $A \rightarrow B \rightarrow C \rightarrow A$ :  
This arises from the fixed point  $p$ , on the left, in the train track.
- $D \rightarrow D$ :  
This loop in the directed graph corresponds to a fixed point located within the edge  $m+2$  in the train track.
- $D \rightarrow E \rightarrow D$ :  
This arises from the fixed point  $q$ , located on the right.
- $A \rightarrow E \rightarrow D \rightarrow C \rightarrow A$ :  
This arises from the sole puncture cycle induced by this train track map, shown below.

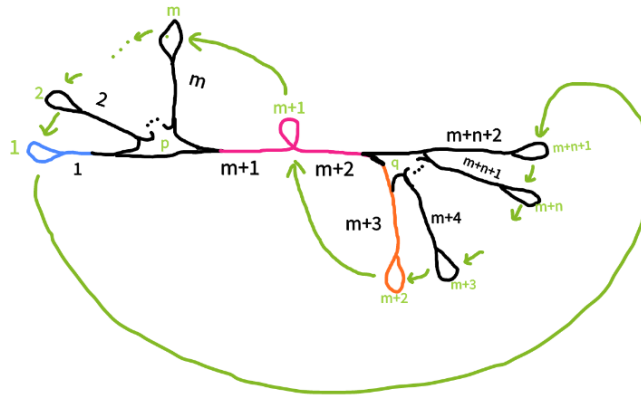
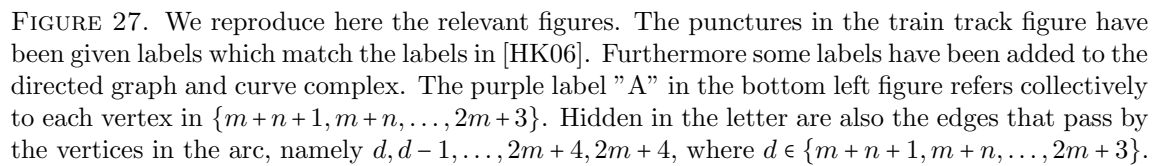


FIGURE 26. The sole puncture cycle.

Next, we consider  $\sigma_{m,n}$ . The relevant figures are reproduced again below:



Here is the sole puncture cycle in this train track, with the punctures labeled and the cycle made explicit with green arrows:

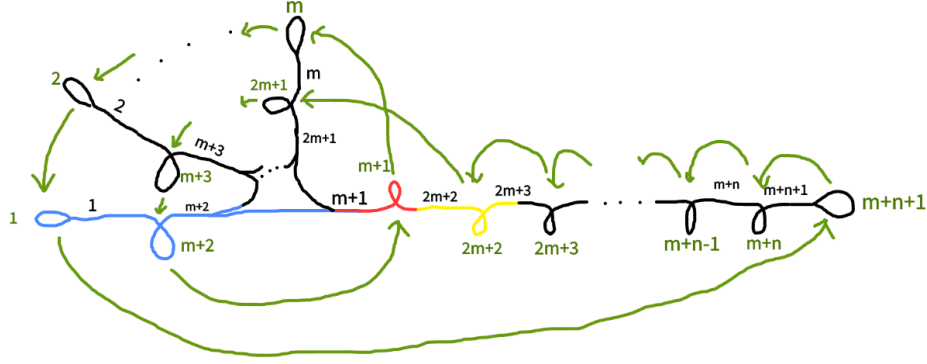


FIGURE 28

- $F \rightarrow E \rightarrow F$ :  
This curve arises from the only rotated fixed point present in the train track.
- $d \rightarrow d-1 \rightarrow \dots \rightarrow 2m+4 \rightarrow 2m+3 \rightarrow D \rightarrow C \rightarrow B \rightarrow d$ :  
Where the vertex label  $d \in \{m+n+1, m+n, \dots, 2m+3\}$  in this context. This curve is induced by the puncture cycle, which is shown in the figure above.
- $B \rightarrow D \rightarrow C \rightarrow B$ :  
This also arises from the puncture cycle. It is one of the induced subcycles.

We make some remarks. The longest puncture cycle has length  $m+n+1$ , and passes through every puncture in the train track. However, there is no directed graph curve of this length because the directed graph cycle that this puncture cycle induces contains multiple copies of a sub-cycle, namely the one that crosses the cyclic sequence of edges  $m, m-1, \dots, 2, 1, 2m+2, m$ .

## REFERENCES

- [HK06] Eriko Hironaka and Eiko Kin. A family of pseudo-anosov braids with small dilatation. *Algebraic & Geometric Topology*, 6(2):699–738, 2006.
- [Iva88] Nikolai V Ivanov. Coefficients of expansion of pseudo-anosov homeomorphisms. *Zap. Nauchn. Sem. Leningrad. Otdel. Mat. Inst. Steklov.(LOMI)*, 167(6):111–116, 1988.
- [McM15] Curtis T McMullen. Entropy and the clique polynomial. *Journal of Topology*, 8(1):184–212, 2015.
- [Tsa24] Chi Cheuk Tsang. Mat993v: Pseudo-anosov maps, 2024.